

Journal of Materials Chemistry C

Accepted Manuscript



This is an *Accepted Manuscript*, which has been through the Royal Society of Chemistry peer review process and has been accepted for publication.

Accepted Manuscripts are published online shortly after acceptance, before technical editing, formatting and proof reading. Using this free service, authors can make their results available to the community, in citable form, before we publish the edited article. We will replace this *Accepted Manuscript* with the edited and formatted *Advance Article* as soon as it is available.

You can find more information about *Accepted Manuscripts* in the [Information for Authors](#).

Please note that technical editing may introduce minor changes to the text and/or graphics, which may alter content. The journal's standard [Terms & Conditions](#) and the [Ethical guidelines](#) still apply. In no event shall the Royal Society of Chemistry be held responsible for any errors or omissions in this *Accepted Manuscript* or any consequences arising from the use of any information it contains.

One-Pot Synthesis of Hydrophilic CuInS₂ and CuInS₂/ZnS Colloidal Quantum Dots

Cite this: DOI: 10.1039/x0xx00000x

Jianbing ZHANG,^{a, b} Weipeng SUN,^a Liping YIN,^a Xiangshui MIAO^{a, b} and Daoli ZHANG,^{a, b, *}

Received 00th January 2012,
Accepted 00th January 2012

DOI: 10.1039/x0xx00000x

www.rsc.org/

A green method for the one-pot direct synthesis of hydrophilic CuInS₂ and CuInS₂/ZnS colloidal quantum dots was developed employing N, N-Dimethylformamide (DMF) as a solvent. Highly reactive H₂S gas, *in situ* generated from the reaction between FeS and H₂SO₄, was utilized as the sulphur source for the synthesis of hydrophilic CuInS₂ quantum dots. Short chain thiols were applied as ligands, reactivity controllers and sulphur sources for the growth of ZnS shell. The growth of CuInS₂ quantum dots experiences a typical Ostwald ripening process, and it should be controlled in 45 min due to the pyrolysis of the ligands. The reaction temperature should not exceed 130 °C. ZnS shell was grown on CuInS₂ quantum dots in a very simple and one-pot approach. Both the luminescence and optical stability were improved substantially after the formation of ZnS shell. The versatility of this synthetic strategy was demonstrated by extending it to the synthesis of other metal sulphide quantum dots, for instance, CdS and ZnS quantum dots.

Introduction

With the development of synthetic chemistry of colloidal quantum dots, colloidal semiconductor quantum dots are being applied in an increasing number of fields, however most of them are cadmium- or lead-containing materials due to ease of synthesis. Considering environment-friendly applications, “greener” colloidal quantum dots are required. InP and CuInS₂ colloidal quantum dots are two important alternatives, and their emission covers the visible and near-infrared windows. The applications of InP colloidal quantum dots are substantially limited because of difficulty in their synthesis,^{1,2} so most recent work focuses on CuInS₂ colloidal quantum dots, including controlled synthesis^{3–8} and the applications in solar cells,^{9,10} light-emitting diodes^{11,12} and biological imaging.^{4,13}

Since Peng³ and Reiss⁴ prepared high quality CuInS₂ colloidal quantum dots using thiols as the reactivity-controlling ligands in a high boiling point solvent, it has become a general synthetic strategy for this class of colloidal quantum dots.^{3,7,11,14} However, CuInS₂ colloidal quantum dots synthesized by this approach are coated with hydrophobic long-chain ligands, which limits their application in many fields. Especially, the hydrophobicity of CuInS₂ quantum dots blocks the application in white light-emitting diodes, in which the quantum dots are employed as colour converters and should be encapsulated into polar polymers, such as silicones. Nevertheless, the hydrophobic ligands with long carbon chains act as polymer softeners and reduce the compatibility with polar polymers^{11,15}. Therefore hydrophilic CuInS₂ colloidal quantum dots are desirable for their extensive applications, and some researchers have managed to obtain hydrophilic CuInS₂ colloidal quantum dots *via* ligand-exchange.^{4,11,13,16} Obviously, the ligand-exchange adds a further complication to preparation processing, and moreover it also cuts down the photoluminescence (PL) quantum yield of CuInS₂

colloidal quantum dots.^{11,15,17} Consequently, directly synthesized hydrophilic CuInS₂ colloidal quantum dots are favourable for their applications.

Generally, hydrophilic colloidal quantum dots are synthesized in aqueous solutions using water-soluble thiols with short chain as capping agents.¹⁸ However, we found that this aqueous method is not suitable for the synthesis of hydrophilic CuInS₂ colloidal quantum dots. Based on our previous work,¹⁹ in which *in situ* generated AsH₃ was used as the arsenic source for the synthesis of InAs colloidal quantum dots, we succeeded in the direct synthesis of hydrophilic CuInS₂ and CuInS₂/ZnS colloidal quantum dots using *in situ* generated H₂S as the sulphur source and highly polar N, N-Dimethylformamide (DMF) as the solvent.²⁰

As proved by Peng *et al.*,³ balancing the reactivity of two cationic precursors is the key to successful synthesis of ternary compound quantum dots. Because the copper carboxylate is too reactive than the indium carboxylate, we used short chain thiols, which were also served as ligands and sulphur source for the growth of ZnS shell, to suppress the reactivity of copper precursor. Different reaction parameters were investigated to optimize the synthetic chemistry. In order to improve the photoluminescence performance of CuInS₂ colloidal quantum dots, we introduced ZnS shell in a simple, one-pot route. The optical stability of hydrophilic CuInS₂ and CuInS₂/ZnS quantum dots were investigated. In addition, preliminary synthesis of CdS and ZnS colloidal quantum dots succeeded *via* this approach (Supporting Information), indicating the versatility of this synthetic strategy for other hydrophilic metal sulphide colloidal quantum dots.

Experimental Section

Chemicals. Indium acetate ($\text{In}(\text{Ac})_3$) (99.99%), 3-mercaptopropionic acid (MPA) (99%), and iron(II) sulphide powder (FeS) (99%) were purchased from Alfa Aesar. Copper(II) acetate monohydrate ($\text{Cu}(\text{Ac})_2 \cdot \text{H}_2\text{O}$) (A. R.), zinc acetate dihydrate ($\text{Zn}(\text{Ac})_2 \cdot 2\text{H}_2\text{O}$) (A. R.), and DMF (99.5%) were purchased from Sinopharm Chemical Reagent Co., Ltd. 1-thioglycerol (TG) (95%) was purchased from Aladdin. All the chemicals were used without further purification. H_2S generated from the reaction between FeS and H_2SO_4 was used as the sulphur source for the growth of CuInS_2 quantum dots. The H_2S was dried prior to use and was handled carefully because of its toxicity.

Synthesis of Hydrophilic CuInS_2 Colloidal Quantum Dots.

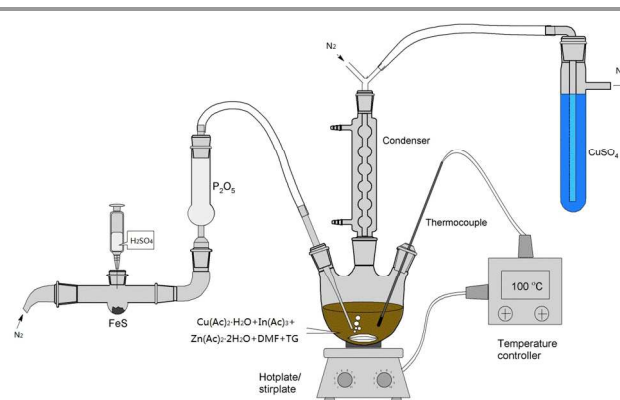
The synthesis is a modification of our previous method¹⁹. For a typical synthetic reaction, 0.2 mmol $\text{In}(\text{Ac})_3$, 0.2 mmol $\text{Cu}(\text{Ac})_2 \cdot \text{H}_2\text{O}$, and 15 mL of DMF were loaded into a three-neck flask. This mixture was heated to 40 °C. When the $\text{Cu}(\text{Ac})_2 \cdot \text{H}_2\text{O}$ was dissolved and the solution became blue, 2 mmol TG was injected into the reaction solution (The TG can also be introduced at the beginning of reaction or after Cu and In precursors are already dissolved). Upon the injection, the colour of the solution changed to slight yellow quickly. Then the temperature of the reaction solution was raised further and the $\text{In}(\text{Ac})_3$ was dissolved slowly. After the reaction solution became transparent and light yellow, the solution was set at a desired reaction temperature, such as 120 °C. Then H_2S , *in situ* generated from the reaction between 0.4 mmol FeS and excess 1 mol/L H_2SO_4 and dried by P_2O_5 , was bubbled into the reaction mixture under N_2 flow. At various time intervals, aliquots of the reaction mixture were withdrawn and diluted in DMF to monitor the evolutions of optical spectra. The solution was cooled to room temperature at the end of the synthetic processing. The whole experiment was carefully operated in a fume hood and residual H_2S was absorbed with CuSO_4 or NaOH aqueous solution. The experimental setup is schematically shown in Scheme 1.

Synthesis of Hydrophilic $\text{CuInS}_2/\text{ZnS}$ Core/Shell Quantum Dots.

In the above synthesis, when H_2S gas was bubbled for ~5 min, 1 mmol $\text{Zn}(\text{Ac})_2 \cdot 2\text{H}_2\text{O}$, which was dissolved in 1 mL DMF, was injected into the reaction mixture. Two hours later, the temperature was raised to 140 °C and was maintained for another 3 hours. After the addition of zinc source, 0.1 mL TG was injected into the reaction flask every hour.

Optical Stability of Hydrophilic CuInS_2 and $\text{CuInS}_2/\text{ZnS}$ Colloidal Quantum Dots. The as-prepared quantum dots were dispersed in DMF and were sealed in air. Hydrophilic CuInS_2 quantum dots were stored uncovered and in dark respectively to distinguish the effect of light on the optical stability. Photoluminescence spectra of CuInS_2 and $\text{CuInS}_2/\text{ZnS}$ colloidal quantum dots were obtained regularly to monitor the evolution of the luminescence performance.

Characterization of Hydrophilic CuInS_2 and $\text{CuInS}_2/\text{ZnS}$ Colloidal Quantum Dots. Absorption and photoluminescence spectra were measured on a Perkin-Elmer Lambda 35 UV-vis spectrometer and a Jasco FP-6500 fluorescent spectrometer respectively. In the optical measurements, DMF is used as the dispersing solvent without adjusting the pH value although the as-prepared quantum dots can be easily dissolved in high purity water. The high purity water will deteriorate and be contaminated easily in air while DMF is much more stable. The quantum yields of the quantum dots were estimated by comparison with ethanol solution of Rhodamin 6G. Powder X-ray diffraction (XRD) patterns were collected on a PANalytical X'Pert PRO. X-ray fluorescence (XRF) spectrum was collected on an EDAX EAGLE III XRF spectrometer. Transmission electron microscopy (TEM) images were obtained on a FEI Tecnai G2 20 transmission electron microscope operating at an accelerating voltage of 200 kV. Generally, hydrophilic quantum dots



Scheme 1 Experimental setup for the synthesis of hydrophilic CuInS_2 and $\text{CuInS}_2/\text{ZnS}$ colloidal quantum dots

have low adhesion to the carbon-coated copper grid, so a moderate amount of alcohol was added into the quantum dots dispersing solution prior to the deposition of the quantum dots on the carbon-coated copper grid.

Results and Discussion

The Influences of Ligands on the Growth of Hydrophilic CuInS_2 Colloidal Quantum Dots. In the synthesis of colloidal quantum dots, ligands are very critical,²¹ which stabilize quantum dots and determine the dispersive nature (hydrophilic or hydrophobic). For one-pot direct synthesis of hydrophilic quantum dots, short chain thiols are usually utilized as the ligands. Nevertheless, the short chain thiols are unstable, and they hydrolyze/pyrolyze partially and release sulphur slowly at a relatively high temperature. Therefore, in the growth of ZnS shell, a ligands, TG, was supplemented regularly. Although the hydrolysis/pyrolysis of these thiols impacts the growth of hydrophilic colloidal quantum dots, the sulphur released from them can be used as a sulphur source to grow sulphur-containing colloidal quantum dots. So in our synthesis, TG was used as the sulphur source to grow ZnS shell while *in situ* generated H_2S was used as the sulphur source to grow hydrophilic CuInS_2 quantum dots. The generation rate of H_2S is difficult to control, and ZnS will nucleate independently if H_2S is applied to grow ZnS shell. Therefore, the ligands are crucial to successfully synthesize hydrophilic CuInS_2 and $\text{CuInS}_2/\text{ZnS}$ colloidal quantum dots. The ligands play three important roles, i. e. (i) stabilizing the as-synthesized colloidal quantum dots and providing solubility in water; (ii) acting as the sulphur sources for the growth of ZnS shell; and (iii) balancing the reactivities of indium and copper sources.

We had investigated several short chain thiols, involving 3-Mercaptopropionic acid (MPA), mercaptosuccinic acid, L-cysteine, thioglycolic acid, and TG, but only MPA and TG are feasible to synthesis of hydrophilic CuInS_2 colloidal quantum dots. The absorption and photoluminescence spectra of CuInS_2 quantum dots synthesized with the same amount of MPA and TG are shown in Figure 1. Not surprisingly, the absorption spectra do not show well-defined exciton absorption peaks, which can be attributed to irregular composition distribution among different quantum dots or large distribution of size/shape.³ The absorption onsets are identical despite the two different ligands are used, indicating that both of them result in quantum dots with the same size. However, TG may lead to a higher experimental yield, which is proved by higher absorption (hence concentration of quantum dots). The same position of the two photoluminescence peaks confirmed the same

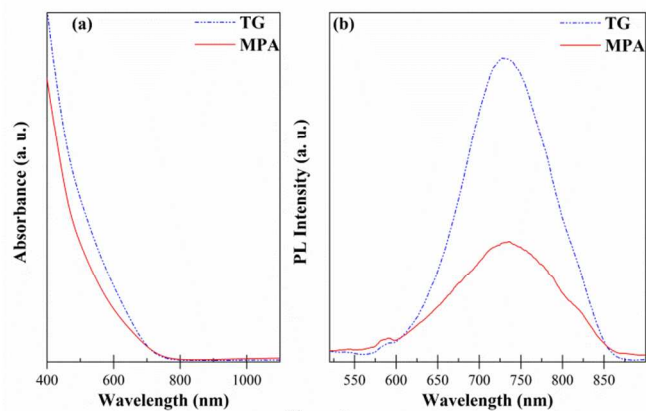


Fig. 1. Absorption (a) and photoluminescence (b) spectra of hydrophilic CuInS_2 quantum dots synthesized with TG and MPA.

size of the quantum dots synthesized with different ligands. Additionally, the quantum dots synthesized employing TG exhibit a much higher photoluminescence intensity, suggesting TG gives rise to a higher photoluminescence quantum yield even the concentration of quantum dots is accounted.

The Influences of Reaction Time on the Growth of Hydrophilic CuInS_2 Colloidal Quantum Dots.

Figure 2 shows the temporal evolution of absorption and photoluminescence spectra of hydrophilic CuInS_2 quantum dots. There is no remarkable change in the absorption spectra from 10 to 45 min, indicating that the CuInS_2 quantum dots were already formed in the first 10 min. On the contrary, the photoluminescence spectra change substantially during 10–45 min. There are two well-defined photoluminescence peaks in a PL spectrum and the relative intensities of them vary as the growth of the quantum dots. From 10 to 20 min, the PL peak at 754 nm enhances and red shifts to 764 nm, while the PL peak at 562 nm diminishes substantially. These two PL peaks can be assigned to two groups of quantum dots due to two nucleation events during the introduction of H_2S gas. When the quantum dots were maintained at a high temperature (120°C), the group of small quantum dots dissolved slowly, indicated by the diminishment of the peak at 562 nm, and release monomers, while the group of large quantum dots grew by absorbing the released monomers demonstrated by the red shift of the peak at 754 nm. When the small quantum dots were dissolved completely (30–60 min), indicated by the disappearance of the PL peak at 562 nm, the PL peak position of the large quantum dots maintained while the PL enhanced due to annealing of the surface. The desolation of the small quantum dots and growth of the large ones indicates the growth of CuInS_2 colloidal quantum dots experience typical Ostwald ripening.²² As shown in Figure 2b, the Ostwald ripening completed in 30 min, and the subsequent heating annealed the surface of the quantum dots and enhanced their photoluminescence performance. However, when the CuInS_2 colloidal quantum dots were heated for 60 min, the photoluminescence intensity only increases slightly while substantial change appears in the absorption

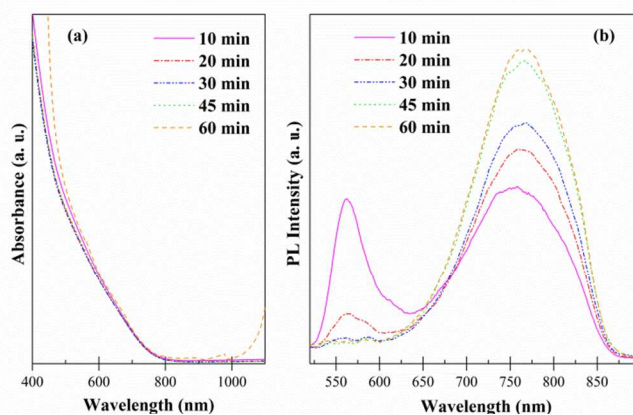


Fig. 2. Temporal evolution of absorption (a) and photoluminescence (The quantum dots were excited at 500 nm) (b) spectra of hydrophilic CuInS_2 quantum dots when they were maintained at 120°C .

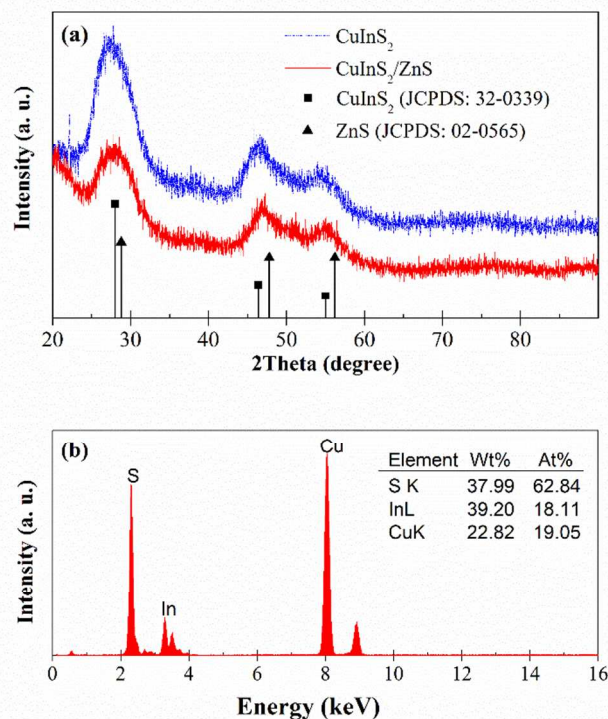


Fig. 3. (a) XRD patterns of hydrophilic CuInS_2 and $\text{CuInS}_2/\text{ZnS}$ quantum dots. (b) XRF spectrum of CuInS_2 quantum dots.

spectrum. The absorption spectrum exhibits remarkable absorption at wavelength larger than 1000 nm, implying the formation of Cu_xS particles³ which may due to the partial pyrolysis of the capping ligands (TG). Consequently, the growth of hydrophilic CuInS_2 colloidal quantum dots shouldn't exceed 45 min.

The XRD pattern of CuInS_2 quantum dots is shown in Figure 3a. The diffraction peaks match well with the standard peaks of bulk CuInS_2 , and there is no any other peak, indicating the phase purity of cubic structure of CuInS_2 quantum dots. The chemical composition (Figure 3b) of the resulting quantum dots

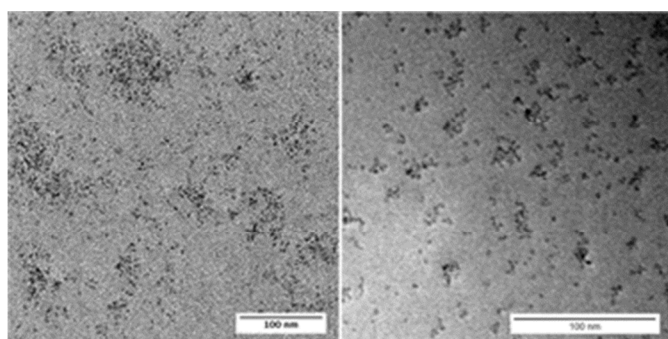


Fig 4 TEM images of CuInS_2 (left) and $\text{CuInS}_2/\text{ZnS}$ (right) quantum dots. The average size (diameter) of CuInS_2 quantum dots is 2.20 nm with a size distribution of 21% (50 particles were counted). The average size of $\text{CuInS}_2/\text{ZnS}$ quantum dots is 3.09 with a size distribution of 18.4% (50 particles were counted).

confirms the formation of CuInS_2 quantum dots. The atomic content of sulphur is higher than 50%, which can be attributed to the sulphur in the capping ligands (TG). Figure 4 shows the TEM image of the CuInS_2 quantum dots. It can be seen that the quantum dots are dispersive and nearly spherical. The large size distributions may account for the indistinguishable absorption peaks of the quantum dots.

Optimization of the Synthesis of Hydrophilic CuInS_2 Colloidal Quantum Dots. In order to optimize the synthetic chemistry of hydrophilic CuInS_2 colloidal quantum dots, the effects of the reaction temperature and the amount of TG were investigated systematically. As shown in Figure 5a, the size of the resulting quantum dots increases with the reaction temperature. The peak positions in the photoluminescence spectra (as shown in Figure 5b) confirm this phenomenon except that of quantum dots prepared at 140 °C. The photoluminescence intensity increases with the temperature from 80 °C to 130 °C while it decreases at 140 °C. The increase of the photoluminescence intensity is due to better passivation of surface at higher temperature, and the decrease can be ascribed to poor passivation due to pyrolysis of TG at high temperature. What's more, there is luminescence below 600 nm in the photoluminescence spectra of the CuInS_2 quantum dots prepared at temperature no less than 130 °C, and its intensity increases quickly with the reaction temperature. The luminescence in this band may result from scattering of exciting light by partially agglomeration of hydrophilic CuInS_2 quantum dots because of partially pyrolysis of the ligands (TG). From this point of view, the pyrolysis of TG already takes place at 130 °C, suggesting the reaction temperature should be controlled below 130 °C.

The ligands serve as stabilizer except the part used as reactivity controller, therefore the concentration of quantum dots decreases as the amount of TG increases (as shown in Figure 5c). When the amount is relatively less (0.2 mL), partially agglomeration appeared due to insufficient coating of surface, thus luminescence in the band of below 600 nm can be seen in the photoluminescence spectrum (Figure 5d). When the amount of TG is adequate for coating the quantum dots, such as 0.4 and 0.6 mL, it has no substantial effect on the photoluminescence performance.

The Growth of $\text{CuInS}_2/\text{ZnS}$ Core/Shell Quantum Dots. The sulphur released by the pyrolysis of TG was used as sulphur source for the growth of ZnS shell, avoiding addition of sulphur-source after the formation of CuInS_2 quantum dots, which simplifies the synthesis procedure apparently. After the formation of ZnS shell, the photoluminescence quantum yield of the quantum dots increased substantially from <0.5% to 9%, as shown in Figure 6.

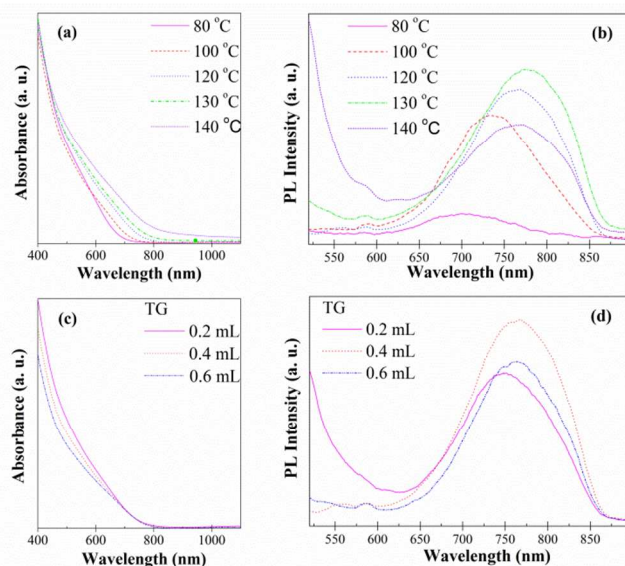


Fig 5. Absorption (a, c) and photoluminescence (b, d) spectra of hydrophilic CuInS_2 quantum dots synthesized at different temperature (a, b) and with different amount of TG (c, d).

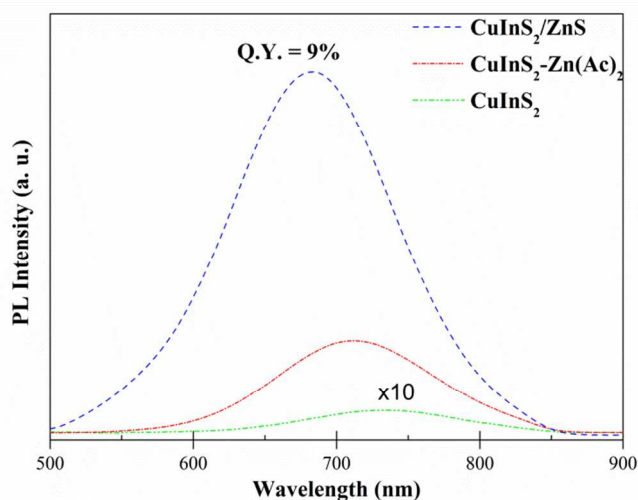


Fig 6. Photoluminescence spectra of CuInS_2 , $\text{CuInS}_2\text{-Zn(Ac)}_2$ and $\text{CuInS}_2/\text{ZnS}$ quantum dots.

The XRD pattern of the $\text{CuInS}_2/\text{ZnS}$ core/shell quantum dots (Figure 3a), in which the three prominent peaks shift to resemble the XRD pattern of ZnS obviously and no mixed peaks of CuInS_2 and ZnS are found, confirms the formation of core/shell structure. Accompanied with the enhancement of the photoluminescence intensity, the peak position shows blue-shift after the shell formation, which has been observed previously.^{4-6,13,14} Surface reconstruction,⁴ zinc diffusion into CuInS_2 core,¹³ cation exchange,¹⁴ etching of the core material,⁶ and a new radiative recombination pathway⁵ were suggested to explain the blue-shift. Taking into account the low temperature of 140 °C during the ZnS growth, this blue-shift may be attributed to surface reconstruction, i. e. suppression of the luminescence of surface states due to the passivation by ZnS shell. In order to verify this point, the photoluminescence spectrum of the quantum dots after the addition

of $\text{Zn}(\text{Ac})_2$, i. e. the quantum dots were capped with TG and $\text{Zn}(\text{Ac})_2$.

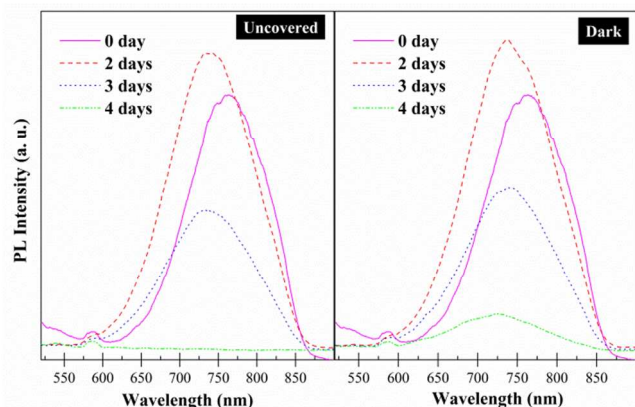


Fig 7. Temporal evolution of photoluminescence spectra of hydrophilic CuInS_2 quantum dots stored uncovered and in dark.

was obtained. The $\text{Zn}(\text{Ac})_2$ can be served as capping ligands to strengthen the luminescence performance,^{20,23,24} demonstrated in Figure 6. Obviously, the peak blue-shifts after the addition of $\text{Zn}(\text{Ac})_2$, confirming that the blue-shift arises from the removal of surface states. In the view of this point, the luminescence of the surface states become a third reason besides the two described previous, which account for the indistinguishable absorption peaks, contributes to the broad photoluminescence peak of CuInS_2 quantum dots.

The Optical Stability of Hydrophilic CuInS_2 and $\text{CuInS}_2/\text{ZnS}$ Colloidal Quantum Dots. Figure 7 shows the temporal evolution of photoluminescence spectra of hydrophilic CuInS_2 quantum dots stored in sunlight and dark. Both the two samples show enhancement of luminescence in the first two days, which can be associated with surface oxidation.^{20,25} When stored for more than two days, the two samples show reduction of luminescence because of excessive surface oxidation. This phenomenon, the photoluminescence intensity increase first and then decrease when it is stored in air, is consistent with the observation of InAs quantum dots.²⁰ Obviously, the light accelerates the oxidation, demonstrated by the spectra obtained on the fourth day.

Figure 8 shows the temporal evolution of photoluminescence spectra of hydrophilic $\text{CuInS}_2/\text{ZnS}$ quantum dots stored uncovered. The photoluminescence intensity decreases monotonously in the first eleven days, and then remains fairly constant after that, exhibiting substantial improvement in optical stability compared to hydrophilic CuInS_2 colloidal quantum dots.

Conclusions

Hydrophilic CuInS_2 and $\text{CuInS}_2/\text{ZnS}$ colloidal quantum dots were directly synthesized using *in situ* generated H_2S as the sulphur source and DMF as the solvent. Short chain thiols were applied as capping ligands, reactivity controlling agents and sulphur sources for the growth of ZnS shell. The investigation on growth kinetics shows the growth of hydrophilic CuInS_2 colloidal quantum dots experienced typical Ostwald ripening and the growth should be controlled in 45 min due to the pyrolysis of the capping ligands. ZnS shell was overcoated on CuInS_2 quantum dots in a very simple and one-pot fashion. The luminescence performance and optical stability of CuInS_2 quantum dots were improved substantially *via* the covering of ZnS shell. The versatility of this synthetic strategy for hydrophilic sulphur-containing colloidal quantum dots was

demonstrated by extending it to the synthesis of other metal chalcogenide quantum dots, for instance, CdS and ZnS quantum dots.

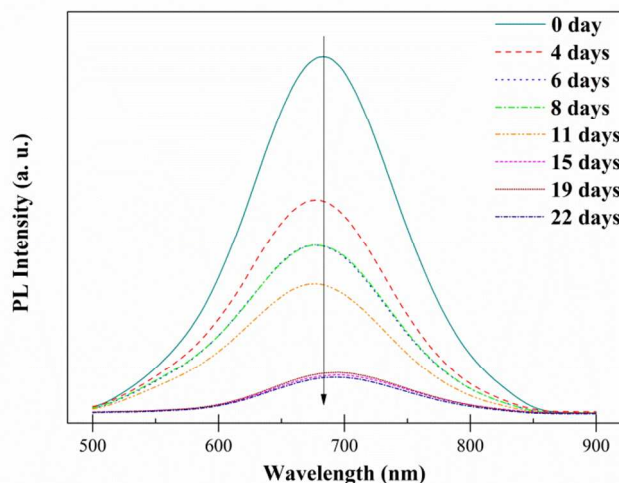


Fig 8. Temporal evolution of photoluminescence spectra of $\text{CuInS}_2/\text{ZnS}$ core/shell quantum dots stored uncovered.

(Supporting Information). The syntheses of these hydrophilic metal sulphide colloidal quantum dots demonstrate the highly reactive H_2S is a good sulphur source and DMF is an alternative solvent besides water. Comparing with water, DMF possesses several advantages for the synthesis of hydrophilic quantum dots, including (i) avoiding the adjustment of the pH value, which is critical for successful synthesis in water; (ii) DMF is much more stable than high purity water which is used in aqueous synthesis; (iii) DMF has higher boiling temperature, making the reaction temperature can be tuned in a larger range thus giving rise to a larger range of control on the size of quantum dots.

Acknowledgements

This work was partially supported by the National Natural Science Foundation of China (NSFC No. 51302096), the Fundamental Research Funds of Wuhan City (No. 2013060501010163), the Fundamental Research Funds of Huazhong University of Science and Technology (No. 2011QN003) and the Graduate Innovation Fund of Huazhong University of Science and Technology (No. HF-11-09-2013). The authors thank Ms Chen Xia and the Analytical and Testing Center of Huazhong University of Science and Technology for the help on measurements.

Notes and references

^a School of Optical and Electronic Information, Huazhong University of Science and Technology, No. 1037 Luoyu Road, Hongshan District, Wuhan City, Hubei Province, 430074, P. R. China. Electronic mail: zhang_daoli@hust.edu.cn

^b Wuhan National Laboratory for Optoelectronics, 1037 Luoyu Road, Hongshan District, Wuhan City, Hubei Province, 430074, P. R. China

Electronic Supplementary Information (ESI) available: Absorption and photoluminescence spectra and XRD patterns of CdS and ZnS quantum dots synthesized via the same approach. See DOI: 10.1039/b000000x/

1 Battaglia, D.; Peng, X. *Nano Lett.* **2002**, *2*, 1027.

2 Li, L.; Protiere, M.; Reiss, P. *Chem. Mater.* **2008**, *20*, 2621.

- 3 Xie, R.; Rutherford, M.; Peng, X. *J. Am. Chem. Soc.* **2009**, *131*, 5691.
- 4 Li, L.; Daou, T. J.; Texier, I.; Kim Chi, T. T.; Liem, N. Q.; Reiss, P. *Chem. Mater.* **2009**, *21*, 2422.
- 5 Nam, D. E.; Song, W. S.; Yang, H. *J. Colloid Interface Sci.* **2011**, *361*, 491.
- 6 Li, L. A.; Pandey, A.; Werder, D. J.; Khanal, B. P.; Pietryga, J. M.; Klimov, V. I. *J. Am. Chem. Soc.* **2011**, *133*, 1176.
- 7 Bao, N. Z.; Qiu, X. M.; Wang, Y. H. A.; Zhou, Z. Y.; Lu, X. H.; Grimes, C. A.; Gupta, A. *Chem. Commun.* **2011**, *47*, 9441.
- 8 Kruszynska, M.; Borchert, H.; Parisi, J.; Kolny-Olesiak, J. *J. Am. Chem. Soc.* **2010**, *132*, 15976.
- 9 Zhou, Z. J.; Fan, J. Q.; Wang, X.; Sun, W. Z.; Zhou, W. H.; Du, Z. L.; Wu, S. X. *ACS Appl. Mater. Interfaces* **2011**, *3*, 2189.
- 10 Rath, T.; Edler, M.; Haas, W.; Fischereder, A.; Moscher, S.; Schenk, A.; Trattig, R.; Sezen, M.; Mauthner, G.; Pein, A.; Meischler, D.; Bartl, K.; Saf, R.; Bansal, N.; Haque, S. A.; Hofer, F.; List, E. J. W.; Trimmel, G. *Adv. Energy Mater.* **2011**, *1*, 1046.
- 11 Kim, H.; Jang, H. S.; Kwon, B. H.; Suh, M.; Kim, Y.; Cheong, S. H.; Jeon, D. Y. *Electrochem. Solid State Lett.* **2012**, *15*, K16.
- 12 Kim, H.; Kwon, B. H.; Suh, M.; Kang, D. S.; Kim, Y.; Jeon, D. Y. *Electrochem. Solid State Lett.* **2011**, *14*, K55.
- 13 Pons, T.; Pic, E.; Lequeux, N.; Cassette, E.; Bezdetsnaya, L.; Guillemin, F.; Marchal, F.; Dubertret, B. *ACS Nano* **2010**, *4*, 2531.
- 14 Park, J.; Kim, S. W. *J. Mater. Chem.* **2011**, *21*, 3745.
- 15 Ziegler, J.; Xu, S.; Kucur, E.; Meister, F.; Batentschuk, M.; Gindele, F.; Nann, T. *Adv. Mater.* **2008**, *20*, 4068.
- 16 Kim, H.; Suh, M.; Kwon, B. H.; Jang, D. S.; Kim, S. W.; Jeon, D. Y. *J. Colloid Interface Sci.* **2011**, *363*, 703.
- 17 Rogach, A. L.; Nagesha, D.; Ostrander, J. W.; Giersig, M.; Kotov, N. A. *Chem. Mater.* **2000**, *12*, 2676.
- 18 Gaponik, N.; Rogach, A. L. *Phys. Chem. Chem. Phys.* **2010**, *12*, 8685.
- 19 Zhang, J. B.; Zhang, D. L. *Chem. Mater.* **2010**, *22*, 1579.
- 20 Rogach, A. L. *Mater. Sci. Eng. B-Solid State Mater. Adv. Technol.* **2000**, *69*, 435.
- 21 Yin, Y.; Alivisatos, A. P. *Nature* **2005**, *437*, 664.
- 22 Ostwald, W. Z. *Phys. Chem.* **1901**, *37*, 385.
- 23 Xu, S.; Ziegler, J.; Nann, T. *J. Mater. Chem.* **2008**, *18*, 2653.
- 24 Li, L.; Reiss, P. *J. Am. Chem. Soc.* **2008**, *130*, 11588.
- 25 Carrillo-Carrión, C.; Cárdenas, S.; Simonet, B. M.; Valcárcel, M. *Chem. Commun.* **2009**, *35*, 5214.